第35卷第12期　　焊　接　学　报　　Vol. 35　No. 12
2014年12月　　TRANSACTIONS OF THE CHINA WELDING INSTITUTION　　December　2014

Sr元素对Al-Si-Zn-xSr钎料组织和性能的影响

刘　晗[1]，　薛松柏[1]，　戴　玮[2]

(1. 南京航空航天大学 材料科学与技术学院，南京　210016; 2. 浙江新锐焊接材料有限公司，嵊州　312452)

摘　要： 研究了Zn，Sr元素对Al-Si-Zn钎料的铺展性能、显微组织、力学性能以及气密性的影响. 结果表明，随着Zn元素含量降低，钎料的铺展面积可增大51%，6061铝合金钎焊接头的强度逐渐升高，达到120.5 MPa. 当加入Sr元素后，钎料的铺展性能得到了显著提升，且随着Sr含量的增加，块状初生硅不断减少，共晶硅由针状转变为点状，并呈网状分布. 当Sr元素质量分数为0.09%时，6061铝合金接头强度最高，为137.1 MPa. 钎焊管路气密性测试结果表明，Al-0.2Si-77.8Zn及Al-2Si-62Zn两种钎料的气密性均逊色于Al-6.5Si-42Zn钎料. 全浸试验后，Al-6.5Si-42Zn钎料的强度降低4.6%，而加入0.09%的Sr元素后钎料的强度降低3.6%.

关键词： 铝硅锌钎料；锶；显微组织；力学性能

中图分类号： TG 425.2　　**文献标识码：** A　　**文章编号：** 0253-360X(2014)12-0093-04

0　序　　言

6061铝合金由于其密度小且具有良好的强度及耐腐蚀性，广泛应用于各种工业结构件，如汽车制造、塔式建筑、船舶、电车、铁道车辆等. 因为其服役环境为多震动、湿热场合，因此焊接接头需具备较高的力学性能和耐腐蚀性能. 钎焊由于焊接变形小、密封性好，接头强度和耐热性能优良，在某些场合成为铝合金件之间连接的首选方法. 目前广泛应用于铝合金钎焊的是传统的Al-12Si共晶钎料，但由于熔点较高(577 ℃左右)而不适用于6061铝合金的钎焊(6061铝合金的固相线温度为583 ℃). 有研究者向Al-12Si合金中添加适量的铜以降低钎料熔点[1,2]，但大约20%的铜加入量才能使钎料熔点降至530 ℃附近，而且大量Cu元素的加入使得接头强度降低，塑性下降，其应用受到限制.

作为铝合金钎焊材料的一个发展方向，Zn元素的加入使得Al-Si-Zn钎料熔点由铝硅共晶温度下降至520 ℃左右[3-5]，具有良好的应用前景. 因此研究Zn元素含量在Al-Si钎料中的影响对Al-Si-Zn钎料的推广应用十分必要. 但是，Al-Si-Zn钎料仍然存在硅相粗大的缺陷，这种相割裂基体，恶化钎焊接头的力学性能[3,4]，尽管目前针对此类问题的解决方法很多，如快速凝固、机械搅拌、超声波振动等，但最直接有效的还是对合金进行变质细化处理. 文中选取锶为变质剂，分析锌，锶含量对Al-Si-Zn-Sr钎料组织和性能的影响.

1　试验方法

1.1　钎料成分设计及制备

试验用钎料采用纯度为99.99%的锌，99.9%的铝，及Al-12Si中间合金铸锭混合熔炼，配制得到不同成分的Al-Si-Zn钎料，再以中间合金Al-10Sr的形式加入锶元素，加入变质剂锶后，保温约1 h并不断搅拌以保证变质剂变质效果良好. 然后冷却，浇铸，分别配制得到的钎料化学成分如表1所示.

表1　钎料合金化学成分(质量分数，%)

Table 1　Chemical compositions of filler metals

合金元素	Zn	Si	Sr	Al
A钎料	77.8	0.2	0	余量
B钎料	62.0	2.0	0	余量
C钎料	42.0	6.5	0	余量
D钎料	42.0	6.5	0.03	余量
E钎料	42.0	6.5	0.06	余量
F钎料	42.0	6.5	0.09	余量
G钎料	42.0	6.5	0.12	余量

将熔炼好的钎料浇铸成ϕ25 mm×1 000 mm的铸棒，去除表面氧化层之后进行挤压并拉拔为直径2 mm的钎料丝，以便于进行6061铝合金的钎焊试验，试验用6061铝合金的成分见表2.

收稿日期：2014-07-30

基金项目：大学生创新训练计划国家级资助项目(201310287043)

表2 试验用6061铝合金化学成分(质量分数,%)
Table 2 Chemical compositions of 6061 aluminum alloy

Si	Mg	Mn	Cr	Zn	Cu	Al
0.61	1.10	0.01	0.12	0.01	0.25	余量

1.2 铺展性能试验

试验母材为6061铝板,试验前先用砂纸打磨,保证试样表面平整、光洁,再进行化学处理去除表面油污,清洗,干燥. 钎料润湿性试验按照国家标准GB/T11364—2008《钎料润湿性试验方法》进行,试样尺寸为40 mm×40 mm×2 mm. 将0.2 g钎料置于6061铝板的中央,覆盖上钎剂,然后将试件平放在试验平台上,平稳的放入箱式电阻炉中,试验温度550 ℃±5 ℃,保温时间1 min. 为了保证试验结果的准确性,每组试样进行五次试验,采用Image-Pro Plus软件计算铺展面积,铺展试验结果取平均值.

1.3 钎焊接头力学性能试验

钎焊接头力学性能试验所用试件为对接钎焊接头,所用试板尺寸为60 mm×25 mm×3 mm. 采用火焰钎焊方法得到6061铝合金的钎焊接头,钎焊接头力学性能测试按照国家标准GB/T11363—2008《钎焊接头强度试验方法》进行,试验加载速率为2 mm/min.

1.4 钎焊接头气密性试验

使用1.2 mm壁厚的6061铝管,钎焊完成后,封闭一端,另一端接气密性检测台接口. 分别测试低压12 MPa及高压21 MPa状态下焊后管路的泄漏现象.

1.5 腐蚀性试验

钎焊接头全浸试验参考国家标准GB10124—88《金属材料试验室均匀腐蚀全浸试验方法》进行,以强度损失速率作为指标考察Al-Si-Zn钎料的耐腐蚀性.

2 试验结果与讨论

2.1 Zn,Sr元素对Al-Si-Zn钎料铺展性能的影响

七种钎料的铺展数据如图1所示. 从图1中可以看出,不加锶时,A,B,C三种钎料的铺展面积随锌含量的降低显著增大. C钎料的铺展面积比A钎料增大51%. 这是因为高温时锌在铝中的固溶度较大,钎料在6061板材上铺展时钎料中的锌以相当快的速度向母材晶间渗透[6],阻碍钎料在6061板材上的铺展. 因此,随着Zn元素含量的降低,液态钎料中锌的浓度降低,向母材内的扩散速度减慢,有利于钎料的铺展. 在C钎料的基础上添加不同含量的Sr元素,Al-Si-Zn-xSr钎料的铺展性能也有大幅提升,且当Sr含量大于0.03%(质量分数)时,铺展面积趋于稳定,此时铺展面积比未添加Sr元素时高出10.5%. 这是因为Sr元素能有效降低液态钎料的表面张力[7],增加钎料的流动性,使铺展性能得到提升.

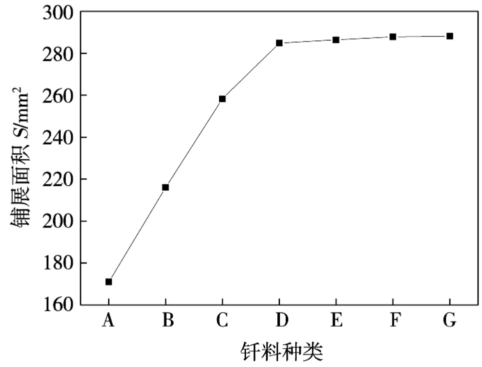

图1 Al-Si-Zn-xSr钎料的铺展面积
Fig. 1 Spread area of Al-Si-Zn-xSr filler metals

2.2 Zn,Sr元素对钎焊组织的影响

图2为A钎料与C钎料的显微组织形貌,由扫描电镜的结果可以清晰地看到A钎料与C钎料中硅相的差异,其中A钎料中没有明显硅相析出,这是因为A钎料中硅含量较低,仅为0.2%(质量分数),室温下可固溶于铝和锌中,因此A钎料的显微组织

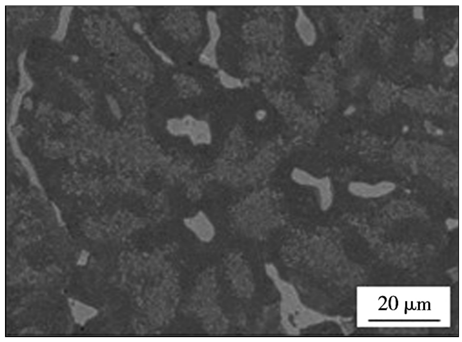

(a) A钎料

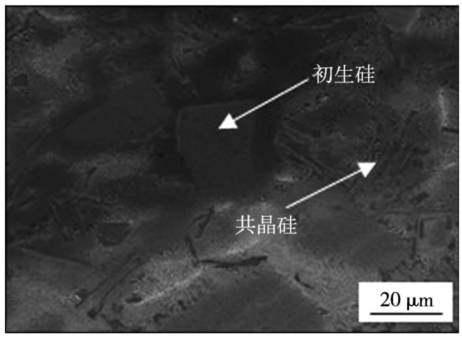

(b) C钎料

图2 Al-Si-Zn钎料的显微组织
Fig. 2 Microstructure of Al-Si-Zn filler metals

与 Zn-22Al 非常相似，而 C 钎料中硅含量较高，为 6.5%（质量分数），比较清晰地出现了大量针状共晶硅，此外还有少量的块状初生硅，且为多边形，边缘清晰.

图 3 为添加 Sr 元素后的钎料显微组织图. 添加微量 Sr 元素后，钎料的组成相没有明显变化（图 4），依旧为锌、铝固溶体与硅相组成，但硅相形貌有较大变化. 当变质元素 Sr 含量为 0.03%（质量分数）时，针状共晶硅已经变为点状，但仍有少量初生硅，同时初生硅的边缘变得模糊，而且有分裂成几小块的迹象. 当 Sr 元素的含量增加到 0.09%（质量分数）时，钎料中的初生硅已基本消失不见，点状的共晶硅连成网状分布，而且共晶硅的颗粒要比 0.03%（质量分数）时更加细小，分布更为均匀. 从未添加 Sr 元素的 C 钎料到完全变质的 F 钎料，钎料中的硅颗粒得到明显细化，数目明显增多，同时钎料中的块状初生硅也随着 Sr 含量的增加而逐渐消失.

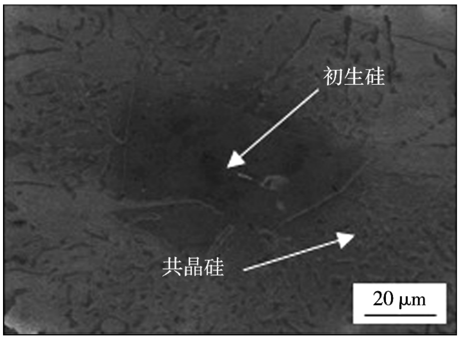

(a) D钎料

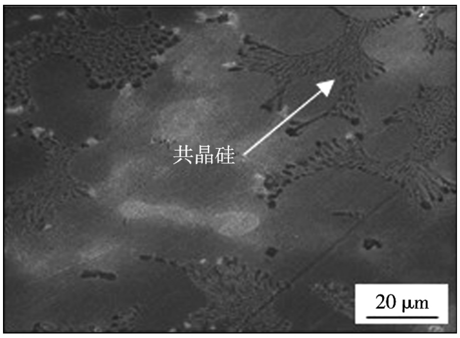

(b) F钎料

图 3　Al-Si-Zn-xSr 钎料的显微组织

Fig. 3　Microstructure of Al-Si-Zn-xSr filler metals

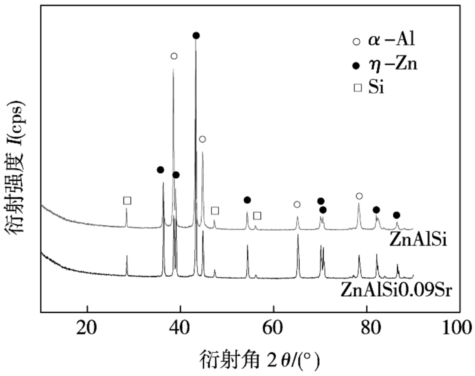

图 4　Al-Si-Zn 钎料 XRD 图谱

Fig. 4　XRD analysis for brazing alloys

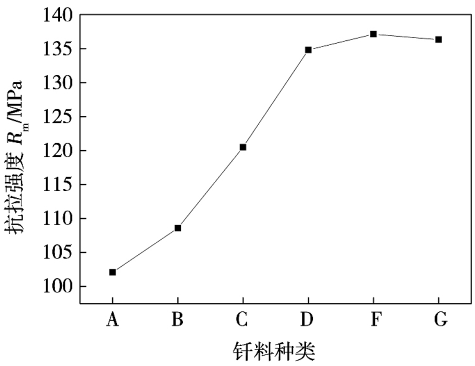

图 5　6061 铝合金钎焊接头抗拉强度

Fig. 5　Tensile strength of 6061 aluminum alloy brazed joints

2.3　Zn，Sr 元素对钎缝力学性能的影响

图 5 为三种 Al-Si-Zn 钎料及三种加锶钎料钎焊 6061 铝合金的强度对比. 由钎焊接头的抗拉强度可以看出，随着 Al-Si-Zn 元素钎料中 Zn 含量的减少，6061 铝合金的接头强度逐渐升高，达到 120.5 MPa. 这与三种钎料铺展面积变化趋势一致.

在 C 钎料的基础上加入微量 Sr 元素，6061 铝合金钎缝抗拉强度得到显著提升，且趋于稳定. 这是因为 Sr 元素作为变质剂起到了优化微观组织的作用. 当 Sr 元素的含量为 0.09%（质量分数）时，钎焊接头的抗拉强度比未变质时高出了约 14%，为 137.1 MPa. 可见钎料微观组织的改善对于提高钎料钎焊接头力学性能有着重要的作用. 当添加少量 Sr 元素时，钎焊接头的力学性能就得到强化，这表明针状共晶硅的转变对钎焊接头力学性能的提升有显著作用.

2.4　Zn，Sr 元素对接头气密性的影响

将 1.2 mm 壁厚的 6061 铝管用 A，B，C，F 钎料焊接完成后进行气密性检测，除 A 钎料外，在低压 12 MPa 状态下，使用其它钎料钎焊后的管路并无泄漏现象出现，当压力达到 21 MPa 时，铝管首先出现破裂，表明钎焊接头的耐压能力高于铝材本身. 因为管路件的使用寿命在很大程度上取决于其抗腐蚀性[8]，故全浸试验之后对铝管进行气密性检测，在试验的 1 000 根铝管接头中，A 钎料的接头未经腐蚀即有 3 根出现泄露. 而对于浸泡 10 天及 30 天之后的 A 钎料钎焊的铝管，泄漏现象更加严重. 对于 B 钎

料钎焊铝管而言，开始时并没有泄漏现象，但浸泡10天之后检漏有4根铝管出现了泄露. 而浸泡30天之后，由于钎料出现的剥落现象，气密性急剧恶化. 由于润湿性能较好，B钎料钎焊铝管泄露的原因应该更多归结于钎焊时的未焊透现象. 这类未焊透现象在浸泡过程中会引起钎料块状脱落，产生裂纹，因此气密性将受到极大影响. 而C，F钎料的接头由于无钎焊缺陷存在，气密性能得到了很大提高，腐蚀试验前后都没有出现泄漏. 同样对全浸试验后的铝板进行拉伸试验，结果如图6所示. A钎料与B钎料钎焊的试件强度损失较大，分别下降16.4%和11.8%，而C钎料与F钎料钎焊的试件在30天之后也仅仅略有降低，分别只下降4.6%和3.6%，但F钎料的抗拉强度较C钎料高出了15%.

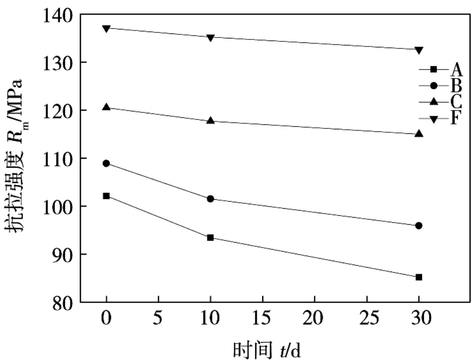

图6 全浸试验后钎焊接头抗拉强度

Fig. 6 Tensile strength of brazed joints after immersion test

3 结 论

(1) 当Al-Si-Zn钎料中Zn元素含量较高时，钎料的流动性较差，适当减少Zn元素的含量，钎料在6061铝合金上的铺展性能明显改善，当Zn元素质量分数为42%时铺展性较佳. 添加少量的Sr元素之后，钎料的铺展性能得到了大幅提升，并且添加质量分数为0.03%的Sr元素即趋于稳定.

(2) Si元素含量较高时，Si元素在Al-Si-Zn钎料中以块状初生硅和针状共晶硅存在. 加入微量Sr元素后，块状初生硅不断减少，共晶硅由针状向点状转变，并在钎料中呈网状均匀分布.

(3) 钎焊接头强度试验结果表明，当Al-Si-Zn钎料中Zn元素含量为42%时，抗拉强度达到最大值120.5 MPa. 当Al-6.5Si-42Zn钎料添加0.09%（质量分数）Sr元素后，抗拉强度提高了约14%.

(4) 气密性试验结果表明，钎焊接头的耐压能力高于铝材本身. 全浸试验后拉伸试验结果表明，Al-6.5Si-42Zn钎料加0.09%（质量分数）Sr元素后抗拉强度提高15%，且强度损失率低于5%.

参考文献:

[1] Chang S Y, Tsao L C, Li T Y, *et al*. Joining 6061 aluminum alloy with Al-Si-Cu filler metals [J]. Journal of Alloys and Compounds, 2009, 488(1): 174－180.

[2] 朱 宏，薛松柏，盛 重. 合金元素对6063铝合金阶梯焊中温钎料性能的影响[J]. 焊接学报，2009，30(8)：33－36. Zhu Hong, Xue Songbai, Sheng Zhong. Effect of alloying elements on intermediate temperature filler metal in stepped welding of 6063 aluminum alloy [J]. Transactions of the China WeldingInstitution, 2009, 30(8): 33－36.

[3] 张 帅，薛松柏，杨金龙，等. P元素对Al-Si-Zn钎料显微组织及性能的影响[J]. 焊接学报，2013，34(5)：103－107. Zhang Shuai, Xue Songbai, Yang Jinlong, *et al*. Effect of P element on microstructure and properties of Al-Si-Zn filler metal [J]. Transactions of the China Welding Institution, 2013, 34(5): 103－107.

[4] 戴 玮，薛松柏，孙 波，等. Cu-P变质对Al-Si-Zn钎料钎缝组织的影响[J]. 焊接学报，2013，34(11)：53－56. Dai Wei, Xue Songbai, Sun Bo, *et al*. Microstructure of Al-Si-Zn filler metal and brazed seam modified with Cu-P [J]. Transactions of the China Welding Institution, 2013, 34(11): 53－56.

[5] Dai Wei, Xue Songbai, Lou Jiyuan, *et al*. Development of Al-Si-Zn-Sr filler metals for brazing 6061 aluminum alloy [J]. Materials and Design, 2012, 42: 395－402.

[6] 张启运，庄鸿寿. 钎焊手册[M]. 北京：机械工业出版社，1998.

[7] Emadi D, Gruzleski J E, Toguri J M. The effect of Na and Sr modification on surface tension and volumetric shrinkage of A356 alloy and their influence on porosity formation [J]. Metallurgical and Materials Transactions B, 1993, 24(6): 1055－1063.

[8] 王 冠，李远波，郭钟宁，等. 汽车散热器新型铝合金钎焊接头腐蚀行为的分析[J]. 焊接学报，2011，32(6)：25－28. Wang Guan, Li Yuanbo, Guo Zhongning, *et al*. Research on corrosion of automobile condenser brazed with novel aluminum alloys [J]. Transactions of the China Welding Institution, 2011, 32(6): 25－28.

作者简介: 刘 晗，男，1993年出生. 本科. 主要从事新型焊接材料及新工艺方面的研究. 发表论文2篇. Email: liuaaun@126.com

通讯作者: 薛松柏，男，博士，教授，博士研究生导师. Email: Xuesb@nuaa.edu.cn

2. School of Materials Science and Engineering, Harbin Institute of Technology at Weihai, Weihai 264209, China; 3. Offshore Oil Engineering (Qingdao) Co., LTD., Qingdao 266520, China). pp 77 – 80

Abstract: The TiN coating were developed on Q235 steel surface by laser cladding using mechanical milling Ti powder. The microstructure of the TiN coating were analyzed by using SEM, XRD EDS and BSE methods. Meanwhile, the hardness, high temperature stability and corrosion resistance of the cladded layers were also measured. The results showed that the TiN coating was composed of TiN, TiO_2 and Fe and a metallurgical bonding was formed. Global particles can be seen in the fusion zone. However, two phases in the form of dendrites and needle platelets were found in the dilution zone. Ti powders can be refined and activated by mechanical milling process. Therefore, finer grain could be easily formed in the coatings by using milled powders. Furthermore, the microhardness and the high temperature stability were excellent. The highest microhardness of the coating was 951.5 MPa under the conditions of laser power 1 000 W and scanning speed 600 mm/min. The corrosion resistance of coating was not good because of the defect like porosity presented in the coating.

Key words: mechanical milling; laser cladding; TiN; microhardness; high temperature stability; corrosion resistance

Asymmetry of inertia friction welding joint LI Jingyong, QIU Shuo, QIU Chenlong (Advanced Welding Technology Provincial Key Laboratory, Jiangsu University of Science and Technology, Zhenjiang 212003, China). pp 81 – 84

Abstract: The temperature fields in inertial friction welded bars, rotating and slipping ones, were measured by thermocouple and wireless temperature-measuring system. The asymmetry of the temperature distribution at both sides of inertial friction interface was investigated. The geometrical feature and macrograph of inertial friction welding zone under different welding conditions were statistically analyzed. It is shown that the temperature and its rising rate at the slipping side are higher than at that one at the rotating side. The axial shortening quantity, flash width and the width of thermal mechanical affected zone (TMAZ) at the slipping side are greater than that one at another side. It is considered that the asymmetry of temperature distributions at both sides of inertial friction interface is closely relevant to the asymmetry of geometrical feature at both sides of the inertial friction welding zone.

Key words: inertial friction welding; temperature field; geometrical feature of welding zones; asymmetry

Dynamic control of mobile robot working in narrow space for weld seam tracking LI Qingwei[1,2] (1. College of Machinery and Electricity Engineering, Xuzhou Institute of Technology, Xuzhou 221008, China; 2. Key Laboratory of Large-scale Engineering Equipment Detection and Control of Jiangsu Province, Xuzhou 221008, China). pp 85 – 88

Abstract: In this paper, a seam tracking control method of a welding mobile robot working in narrow space was studied. A kinematic model of the robot was built for tracking right-angle fillet seams. And based on the newton-euler method, the dynamic behaviors of the driving wheel, the mobile body and the cross slider of the robot were analyzed, and then the overall dynamic model of the robot was obtained. On the basis of a reasonable simplification of the overall dynamic model, a robust PI controller was proposed. The simulation was performed on software Matlab and experiments was carried out. The results show that the proposed controller can complete the scheduled task possessing a high tracking accuracy.

Key words: mobile welding robot; fillet weld; seam tracking; dynamics; robust PI controller

In-situ synthesis of Fe-based ZrC-ZrB$_2$ composite coating produced by GTAW CHEN Lili[1], WANG Zhenting[2], YANG Deyun[1] (1. Department of Materials Engineering, Harbin Huade University, Harbin 150025, China; 2. College of Materials Science and Engineering, Heilongjiang Institute of Science and Technology, Harbin 150027, China). pp 89 – 92

Abstract: A Fe-based composite coating reinforced by ZrC-ZrB_2 particles has been successfully fabricated on Q235 steel by gas tungsten arc welding (GTAW) cladding process utilizing the in situ reaction of pre-placed Zr, B4C and Fe powders. The microstructure of the coating was analyzed by scanning electron microscopy (SEM), X-ray diffraction (XRD), energy-dispersive spectrum (EDS), and the growth mechanism of the ZrC-ZrB_2 reinforcement was discussed. Meantime, the microhardness and the wear resistance of the composite coating were examined by means of microhardness tester and wear tester at room temperature, respectively. The results show that the coating that has excellent metallurgical bonding with substrate can be obtained. The main phases of coating are ZrC, ZrB_2 and α-Fe, in which the ZrC phase exhibits hexahedron and petalled shapes and the ZrC-ZrB_2 compound presents acicular and rod shape. The microhardness of coating is up to 1 200 MPa, and the wear resistance is about twenty times higher than that of the Q235 steel.

Key words: GTAW overlay; in-situ synthesis; microstructure; growth mechanism

Effect of strontium on microstructure and properties of Al-Si-Zn-xSr filler metals LIU Han[1], XUE Songbai[1], DAI Wei[2] (1. College of Materials Science and Technology, Nanjing University of Aeronautics and Astronautics, Nanjing 210016, China; 2. Zhejiang Xinrui Welding Material Co., Ltd., Shengzhou 312452, China). pp 93 – 96

Abstract: The effect of zinc and strontium element on the spreadability, microstructure, and mechanical properties of Al-Si-Zn filler metal has been investigated. The results indicated that the spread area was increased by 51% with decreasing Zn content, and the tensile strength of the brazed 6061 aluminum alloy joint was gradually increased to 120.5MPa. With the addition of Sr, the spreadability of Al-Si-Zn filler metal was significantly improved, the number of primary Si particles decreased and the eutectic Si was changed from acicular to fine fibrous morphology distributed in a netlike form. The strength of 6061 aluminum alloy joint reached the peak value of 137.1 MPa when the content of Sr was 0.09%. The air-tightness test of the brazed pipe showed that the tightness of Al-0.2Si-77.8Zn and Al-2Si-62Zn were inferior to that of Al-6.5Si-42Zn. After the immersion test, the tensile strength of Al-6.5Si-42Zn filler metal was decreased by 4.6%, while the Al-6.5Si-42Zn-0.09Sr filler metal was only by 3.6%.

Key words: Al-Si-Zn filler metal; strontium; microstructure; mechanical properties

Research on microstructure and corrosion resistance of electro-spark overlaying of AZ91D magnesium alloy ZHAO Jianhua[1,2], GAI Rui[1], WANG Zihong[1] (1. College of Materials Science and Engineering, Chongqing University, Chongqing 400044, China; 2. National Engineering Research Center for Magnesium Alloys, Chongqing University, Chongqing 400044, China). pp 97 – 100, 104

Abstract: The overlaying welding was produced on the surface of AZ91D magnesium alloy by electro-spark welding (ESW) technique using an electrode which is as same as the base metal. The microstructure, bonding interface and corrosion resistance of the layer were investigated. The results showed that the ESW process can produce a uniform and dense weld with proper process parameters. The weld microstructure consisted of supersaturated α-Mg solid solution with size of 1 – 5 μm, $Mg_{17}Al_{12}$ phase and metastable AlMg phase. The weld was metallurgically bonded to the base metal and a thin layer formed by inter-diffusion, crystallization was formed at the interface between the weld and base metal. There is no obvious heat affected zone on the side of the base metal and original composition of the electrode material was retained in the weld. The corrosion resistance of weld was better than the base metal. The grain refinement of the weld can improve the uniformity of the corrosion, meanwhile, the supersaturated α-Mg solid solution and β phase that was continuously distributed at the grain boundaries with the a netlike morphology can decrease the corrosion rate, which are the main factors leading to a high corrosion resistance of the weld.

Key words: electro-spark welding; magnesium alloy; microstructure; corrosion resistance

Valence electron structure of brazing joint interface for honeycomb sandwich construction in titanium alloy JING Yongjuan, LI Xiaohong, HOU Baojin, YUE Xishan (Beijing Aeronautical Manufacturing Technology Research Institute, Beijing 100024, China). pp 101 – 104

Abstract: In this paper, the microstructure and the precipitations in the interface were studied for the honeycomb sandwich construction in titanium alloy. The valence electron structure of the brazing joint interface was calculated by the empirical electron theory (EET) in solid and molecules. The inter-atomic binding force was analyzed and the relationship between it and the microstructure was discussed. The $TiNi_3(Cu,Zr)$ -compound with hcp lattice structure and the Ti(Ni,Zr,Cu) solid solution with bcc structure were formed in the welding. The maximum valence electron and maximum crystal electron for the matrix was 0.305 9 and 1.397 3, which represented the ability of the strength and ductility for the crystal respectively. For the $TiNi_3(Cu,Zr)$ compound and the Ti(Ni,Zr,Cu) phase, the maximum valence electron was 0.055 8 and 0.303 7 respectively, and the maximum crystal electron was 0.993 5 and 1.392 8 respectively. Thus, the ability of the strength and ductility for the Ti(Ni,Zr,Cu) phase and the matrix is better than that of the $TiNi_3(Cu,Zr)$ -compound. The discontinuity of the microstructure in the interface is disadvantage for the strength and ductility.

Key words: titanium alloy; brazing joint interface; EET

Prediction of mechanical properties of welding joints by hybrid cluster fuzzy RBF neural network TANG Zhengkui[1], DONG Junhui[1], ZHANG Yongzhi[1,2], HOU Jijun[1] (1. School of Materials Science and Engineering, Inner Mongolia University of Technology, Hohhot 010051, China; 2. Inner Mongolia Guodian Energy Investment Co., Ltd., Electric Power Engineering and Technology Institute, Hohhot 010080, China). pp 105 – 108

Abstract: The build of hybrid clustering algorithmcombined with the pseudo-inverse method was carried out to establish the RBF neural network model to predict the mechanical properties of welded joints. Taking TC4 titanium alloy TIG welding experiments as basis, the welding parameters was set as model input and the mechanical properties of welded joints was set as output. Through simulation, the mean relative error of the predictions ranged from 1.74 to 6.69%, indicating that the model has higher prediction accuracy, adaptability and better generalization ability to predict the mechanical properties of welded joints. The model decomposed by using the mathematical analysis method, can obtain a functional expression between the welding parameters and mechanical properties of the joint process. The welding parameters can also be optimized simultaneously. The utilization of welding professional knowledge was applied to adjust the RBF unit parameter of model, allowing an increase of the prediction accuracy of the model. It has opened a new way to take the welding expert knowledge into the RBF neural network model.

Key words: subtractive clustering; fuzzy c-meaning cluster; radial basis function neural network; welding; modeling

Aluminum stud welding using TIG-arc hybrid heating source ZHANG Deku, WANG Yan, WANG Kehong, KANG Lulu (Department of Materials Science and Engineering, Nanjing University of Science and Technology, Nanjing 210094, China). pp 109 – 112

Abstract: Aiming at the problematic issues occured in stud welding in large diameter component, such as gas pore, hot crack and incomplete fusion and poor joint, a welding technology was proposed using TIG-Arc hybrid heating sourceand conducted on Φ16 mm aluminum stud welding. Before the welding of aluminum stud, immersion plating of Zn-Ni layer was applied on the aluminum stud. The whole welding process was protected with inert gas. The shear strength of joint can reached 128 MPa and the strength coefficient of the joint is above 70%. The optimum welding parameters are, preheating temperature of 200 ℃, welding time of 1000ms, welding current of 650A. The experimental results also show that the pretreatment of aluminum by TIG and Zn-Ni plating of can effectively improve the mechanical properties and the microstructure of the joint.

Key words: aluminum; stud welding; hybrid heating resource; immersion plating